CANARY AND PORTUGAL CURRENTS

E. D. Barton, University of Wales, Bangor, UK

Introduction

The Canary and Portugal Currents form the eastern limb of the North Atlantic Subtropical Gyre. Detailed knowledge of the currents is still surprisingly sparse in some respects and is largely based on indirect methods of estimating the flow. The entire eastern boundary of the gyre is affected by the process of coastal upwelling, driven by the seasonally varying Trade Winds. Upwelling is intimately related to the currents on the continental shelf, and varies on timescales from several days upwards. This phenomenon has been studied intensively at different places and times and long-term sampling has only begun in recent years.

Large-scale Circulation

The low to midlatitudes of the North Atlantic Ocean are occupied by the clockwise rotating subtropical gyre (**Figure 1**). The western boundary of this system is made up by the Gulf Stream, which feeds into the North Atlantic Current and the Azores Current. The latter flows eastward to supply the eastern subtropical boundary region. Branches of the Azores Current loop gently into the Portugal

Current and further south into the Canary Current. The latter separates from the African coast at around 20°N to become the North Equatorial Current, which eventually feeds into the Caribbean Current and back to the Gulf Stream.

Using all available hydrographic data, the long-term average geostrophic flow for the region has been calculated assuming a level of no motion near 1200 m. Scarcity of data limits the resolution of the analysis to a grid of $3° \times 3°$; near the coast, where deep data are even fewer, results are more uncertain. Where the eastward-flowing Azores Current turns south as it nears the eastern boundary, two branches of the Canary Current are formed (**Figure 2A**) separated by Madeira. West of Iberia only weak near-surface flow toward the eastern boundary is indicated, while nearer to shore the Portugal Current carries about $2 \times 10^6 \, m^3 \, s^{-1}$ equatorward in the layers above 200 m depth. Only some of this continues southward into the Canary Current, while the rest apparently enters the Mediterranean in a shallow surface layer. The total amount of water carried equatorward above 200 m in the Canary Current, including input from the Portugal Current, was estimated at about $4 \times 10^6 \, m^3 \, s^{-1}$ between 35°W and the African coast. Near 20°N the Canary Current breaks away from the African coast to turn westward as the North Equatorial Current near 15°N. South of this separation point, a recirculation cell around the 'Guinea Dome' lies east of the Cape Verde Islands between the coast and the equatorward flow.

The Canary Current varies seasonally by slight changes in position but not greatly in transport (**Figure 3**). Areas of larger uncertainty, shaded in the figure, correspond to few or no hydrographic samples in that study. The near-shore branch of the current migrates seasonally across the Canary Islands, closer to Africa in summer and farther offshore in winter. As it does so, the Azores Current oscillates south in summer and north in winter, so that the eastern part of the gyre has an annual 'wobble.' Some streamlines intersect the African coast in the northern half of the area and leave in the south, suggestive of a narrow, intense equatorward flow in the under-sampled coastal band between 20° and 30°N, particularly in spring and summer. Recirculation south of 20°N is clearest in winter and spring, but indications of northward flow are also seen there during other seasons. In autumn, near-shore northward flow extends as far
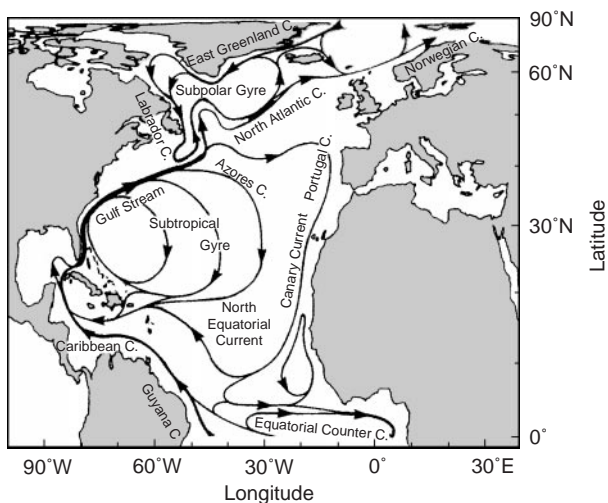
Figure 1 Sketch of the general near-surface circulation of the North Atlantic Ocean.
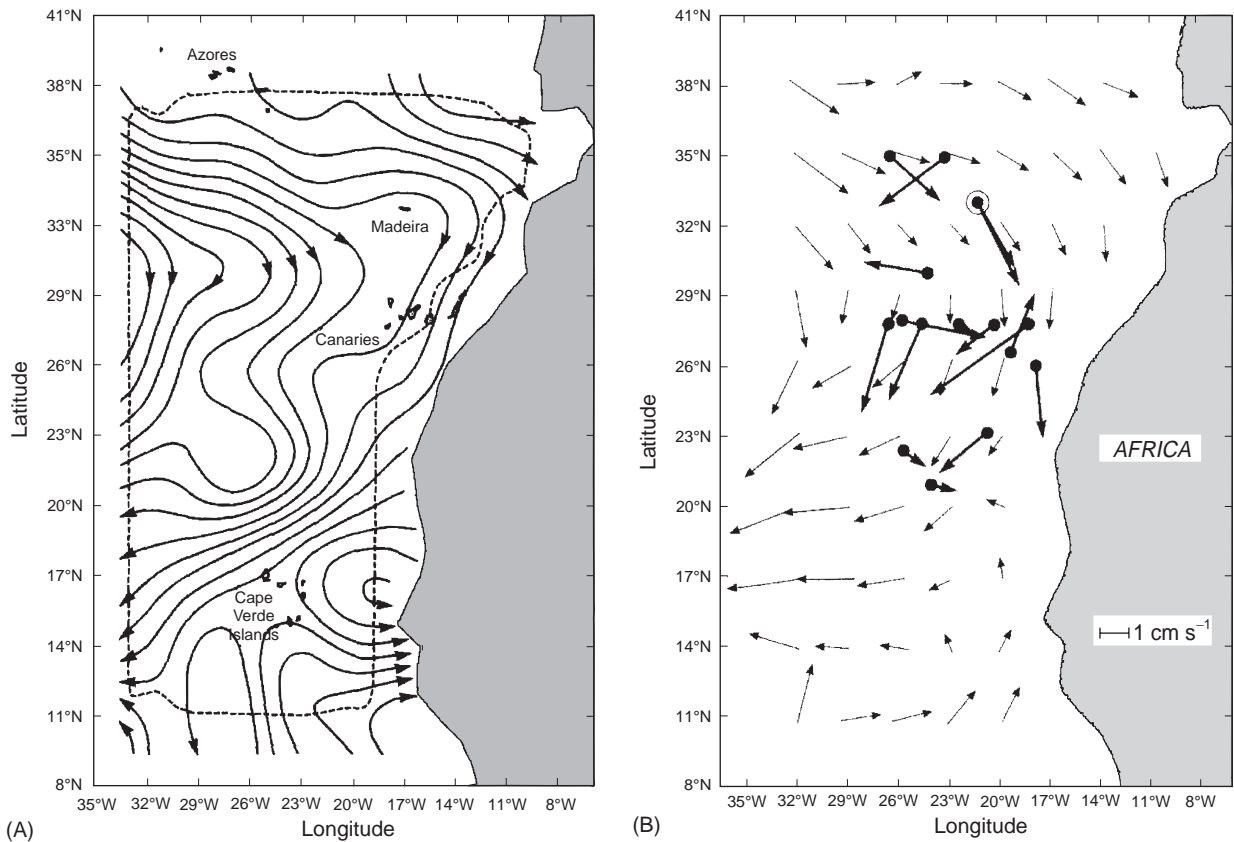
Figure 2 (A) Total transport of volume calculated from the long-term mean density field with the geostrophic assumption and summed from 200 m depth to the sea surface. Between any pair of streamlines the volume transport is $0.5 \times 10^6 \, \text{m}^3 \, \text{s}^{-1}$. The calculations have less uncertainty inside the dashed line. (B) Geostrophic current vectors (thin arrows) at 200 m depth calculated from the long-term mean density field and mean observed currents (thick arrows) near 200 m at the sites marked by dots. The circled dot indicates the longest record, Kiel276.

as the Canaries, although again in the coastal under-sampled band.

The few available long-term moored observations are mainly well away from shore and the shallowest records are at about 200 m depth. Most lasted 1–2 years, but one mooring (Kiel276) is continuous since 1980 on the southern edge of the Azores Current (33°N, 22°W). In general, fluctuations were more than 5 times more energetic than the mean flow and so most records do not provide a reliable statistical estimate of the average. Nevertheless, the measured mean currents agree broadly with the large-scale geostrophic flow (**Figure 2B**) but indicate that the transport may be > 50% more than indicated by the geostrophic calculations. No subsurface record indicated significant seasonal variability. However, the Kiel276 record demonstrated the dominance of meanders and eddies in the Azores Current and variability on the scale of a decade. Since the Azores Current feeds into the eastern boundary system, similar long-term variability likely occurs in the

Canary and Portugal Currents as well, although no long-term current monitoring has yet been achieved there.

Several year-long moorings, deployed recently between the Canary Islands and the African shelf, showed highly variable flow, with maximum velocities near 0.3–0.4 m s^{-1}, but seasonal mean currents 10 times smaller. In mid-channel the upper 200 m layer flowed southward with variable strength. The bulk of the upper 600 m flowed mainly southward in winter and spring, but northward in summer and autumn. Despite increased Trade Winds in summer the Canary Current decreased east of the Canary Islands, at the same time as the flow through the western islands increased. These observations are compatible with the suggested seasonal variation in the gyre and the extension of near-surface poleward flow to the latitude of the Canaries, although the timing is out of phase with the long-term seasonal average results. Of course, any single year is not necessarily representative of the
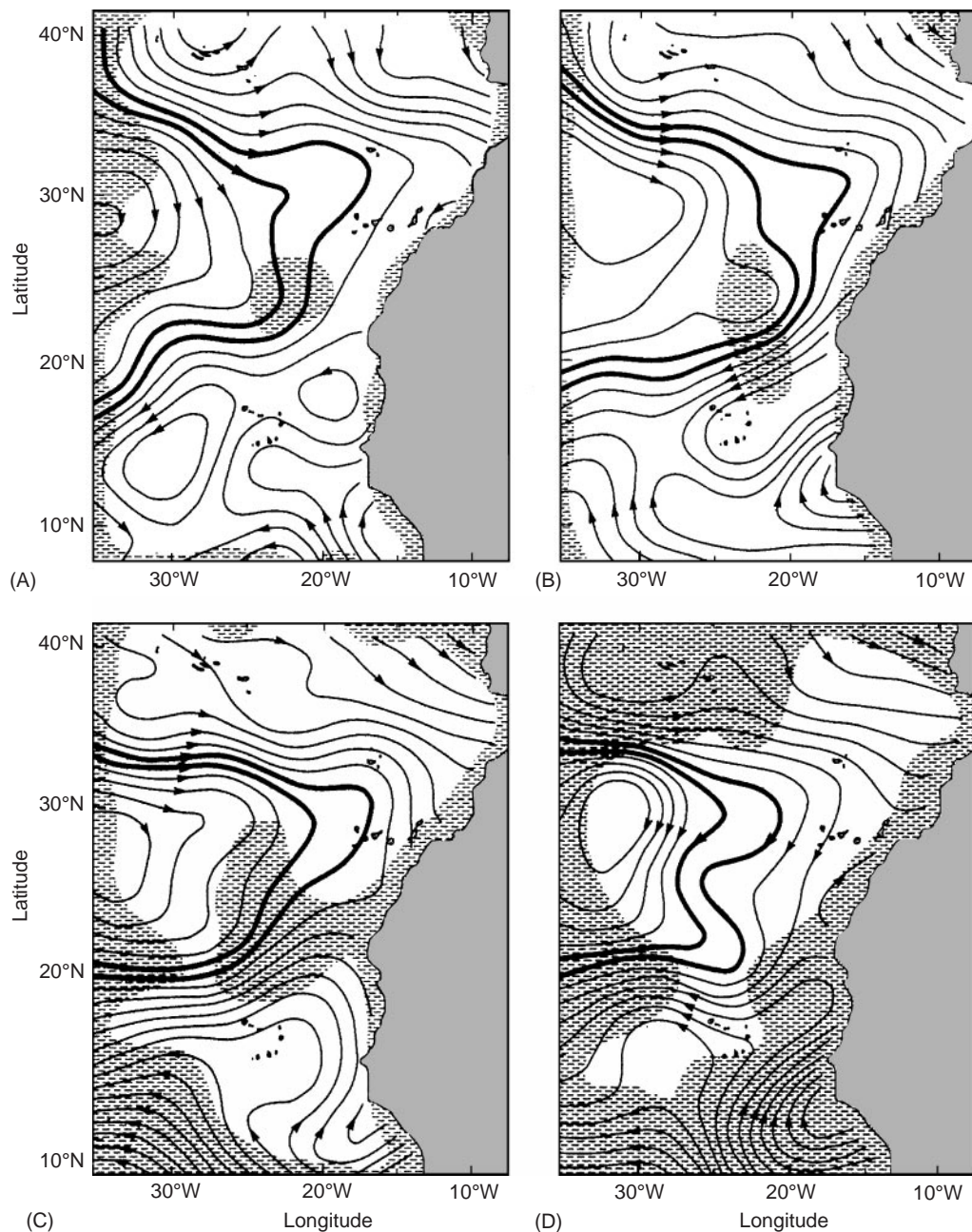
Figure 3 Seasonal variation of the geostrophic volume transport above 200 m depth in the eastern boundary region, calculated as before for (A) spring, (B) summer, (C) autumn, and (D) winter. Areas of larger uncertainty are shaded. Flow between any pair of streamlines is $0.5 \times 10^6 \, \text{m}^3 \, \text{s}^{-1}$.

long-term mean. There was no evidence of strong equatorward flow along the continental margin in spring and summer, though measurements did not extend over the upper slope and shelf.

Coastal Upwelling

For some part of the year the north-east Trade Winds blow along every part of the subtropical Eastern boundary with a strong alongshore component that produces offshore Ekman transport in the surface layers and therefore upwelling at the coast. The strength of upwelling is conventionally expressed in terms of the upwelling (or Bakun) index, which is simply the Ekman transport $T_E = (\tau/\rho f)$ where τ is the component of wind stress parallel to shore, ρ is the density of sea water, and f is the Coriolis parameter. The index is routinely

calculated from coastal surface wind data on a daily or monthly basis. It represents the rate at which water is removed from shore in the surface layer and, in a two-dimensional system, the amount of water upwelled to replace it.

The annual cycle of upwelling for the region (**Figure 4**) shows the coastal temperature anomaly with respect to central ocean alongside the monthly mean upwelling index. Summer Trade Winds affect the

Iberian and African coasts north of 20°N. Off the West Coast of Iberia, upwelling generally starts in May or June and lasts only until September. The southern, Algarve, coast of Portugal and north coast of Morocco (33–37°N) are oriented at a large angle to the Trade Winds and so upwelling there is intermittent and short-lived. In winter the Trades shift southward to provoke upwelling between 30° and 12°N. South of 20°N upwelling starts in December
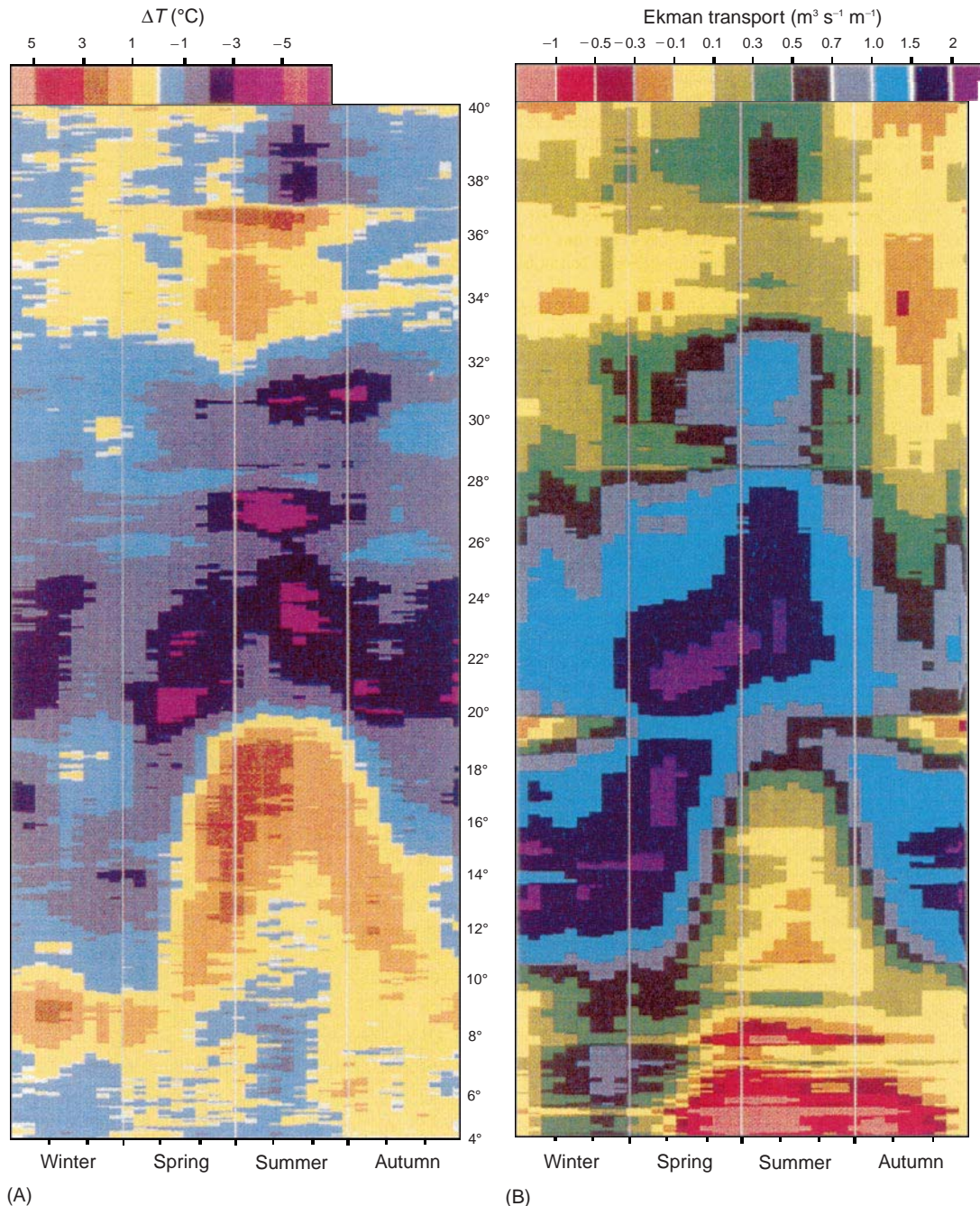

Figure 4 Annual cycle of upwelling represented by (A) temperature difference between the coast and midocean determined by satellite sea surface temperature estimates, and (B) the upwelling index calculated from surface atmospheric pressure analyses.

and lasts until April or May. Between 20° and 30°N the coast is subject to year round upwelling that peaks in July and August.

Wind forcing and strength of upwelling, as represented by coastal temperature anomaly, show variations up to a factor of 2 between years and decades. The 1960s were typified by upwelling of about half of the average intensity off West Africa. Upwelling increased through the 1970s, only to weaken again in the 1980s and increase in the 1990s. An intriguing finding is that the strength of upwelling appears to be increasing in the long term – a trend common to all the upwelling regions of the world over the last 40 years. This may be linked to global warming, because increased summer heating deepens the continental low-pressure systems so increasing the atmospheric pressure difference with the oceanic highs to intensify the Trade Winds.

On short timescales the Trade Winds typically remain nearly constant over periods of 7–10 days and then relax to near zero or weakly northward for several days. Observations over the continental shelf of NW Africa have shown how the system responds (**Figure 5**). Favorable winds drive offshore Ekman transport above about 30 m depth and raise the pycnocline near shore so that within one day colder, less salty subsurface water breaches the sea surface. The upwelled water, which can originate from as deep as 200 m, is denser, and there is a slight downward slope of the sea surface toward the coast because of the offshore transport. These give rise to an equatorward geostrophic flow that weakens with depth over the shelf. The jet is strongest where the pycnocline intersects the surface as a boundary between the denser upwelled waters and the less dense oceanic waters, where it reaches velocities of up to 0.8 m s^{-1} in the example shown. As the wind varies,
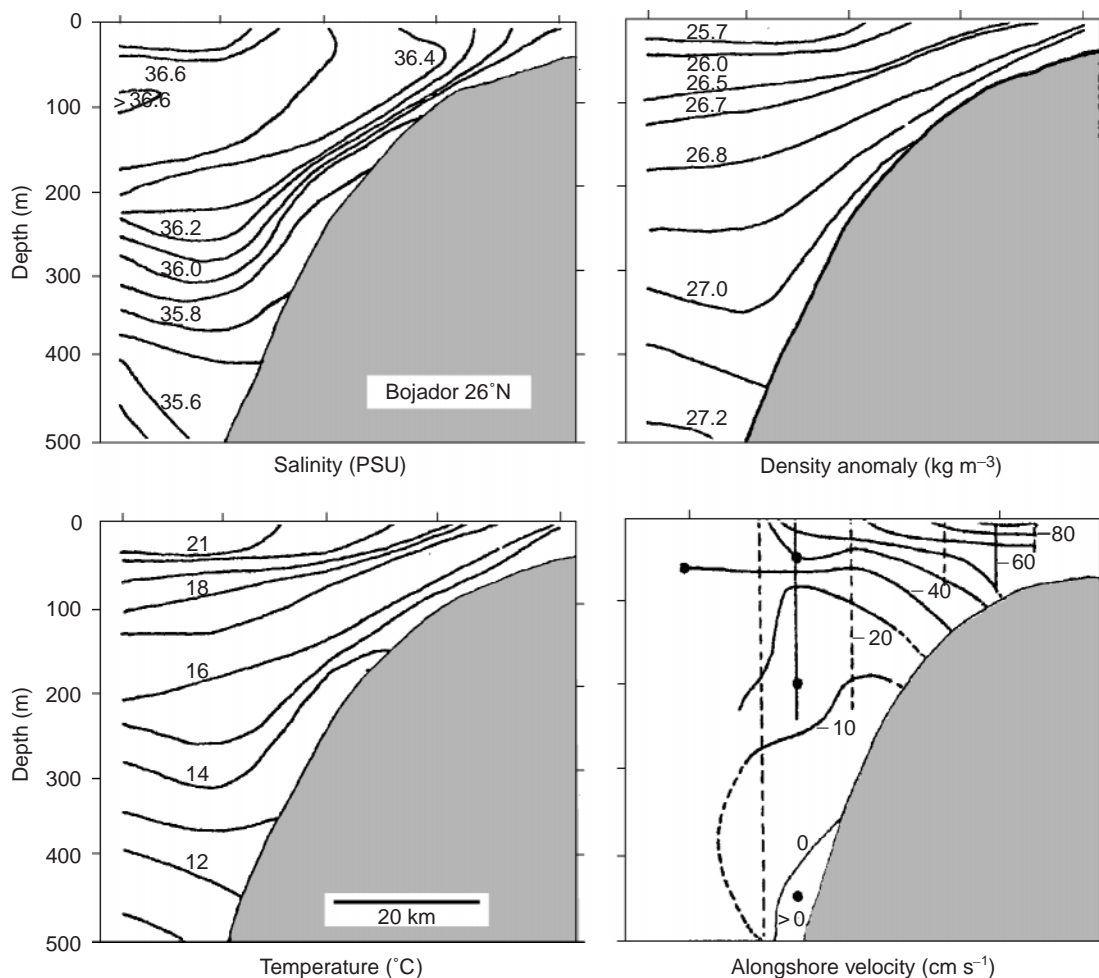
Figure 5   Sections of temperature, salinity, density, and alongshore current off north-west Africa during favorable winds in August. Contours are elevated from ∼ 200 m to the sea surface. The current field is based on a combination of moored current meter (solid dots), profiling current meter (solid vertical lines), and geostrophic estimates (dashed vertical lines).

so do the slopes of the sea surface and the pycnocline, the strength of upwelling, and the speed of the alongshore jet. The scale of the upwelling region, i.e., the distance within which the isosurfaces are uplifted is given by the Rossby radius of deformation $\lambda = \sqrt{(g\Delta\rho/\rho h)}/f$, where g is the gravitational acceleration, h is the undisturbed depth of the surface layer above the pycnocline, ρ is the density of the deep water, and $\Delta\rho$ is the density contrast between the surface and deep layers. The characteristic upwelling velocity, w, is given by the upward transport divided by the width of the upwelling zone $w = T/\lambda$. For a typical situation $\lambda \sim 10\text{–}20\,\text{km}$, and $w \sim 10\,\text{m}\,\text{d}^{-1}$.

The onshore–offshore flow observed off NW Africa conforms to the classic picture of upwelling (**Figure 6**) where the surface layer offshore flow is compensated by deeper onshore flow. When the wind relaxes, the whole water column on the shelf moves shoreward, carrying with it warm oceanic waters. Detailed comparisons of the time-varying offshore and onshore transports with the Ekman index have shown good agreement between offshore flow and the index, in this and other upwelling regions. Poorer agreement is found between offshore and onshore transport, which often appear to be locally out of balance.

Satellite imagery of sea surface temperature fields shows that the boundary between upwelled waters and open ocean is often strongly contorted into long filaments of cooler water stretching hundreds of kilometers out to sea. Filaments identified off the Iberian and African coasts appear to develop from instabilities of the along-frontal flow, often triggered by coastal or topographic irregularities such as capes or ridges. Some appear associated with offshore eddies, which may themselves be topographically anchored. Filaments tend to recur in the same positions year after year, as, for example, the one off north-west Spain at 42°N in **Figure 7**. They are associated with localized areas of net offshore flow (therefore local imbalance in the cross-shelf transport) that take the form of a narrow jet where the alongshore flow is diverted seaward. The figure shows a surface drifter following the filament offshore at a mean rate of $0.3\,\text{m}\,\text{s}^{-1}$. This offshore transport can help effect exchange of water properties between shelf and deep ocean because of mixing along the filament boundary and interaction with the deeper waters beneath. As upwelled waters move offshore in the filaments, they gradually warm and become indistinguishable from surrounding waters so that any return flow to the coast is not easily identified in satellite images.

Poleward Undercurrent

Beneath the near-surface equatorward flow of the Canary Current, a subsurface current flows poleward, counter to the general circulation and tightly bound to the continental slope. It has been documented along the entire continental margin between the Gulf of Guinea and north-west Spain, and is a common feature of all eastern boundaries.
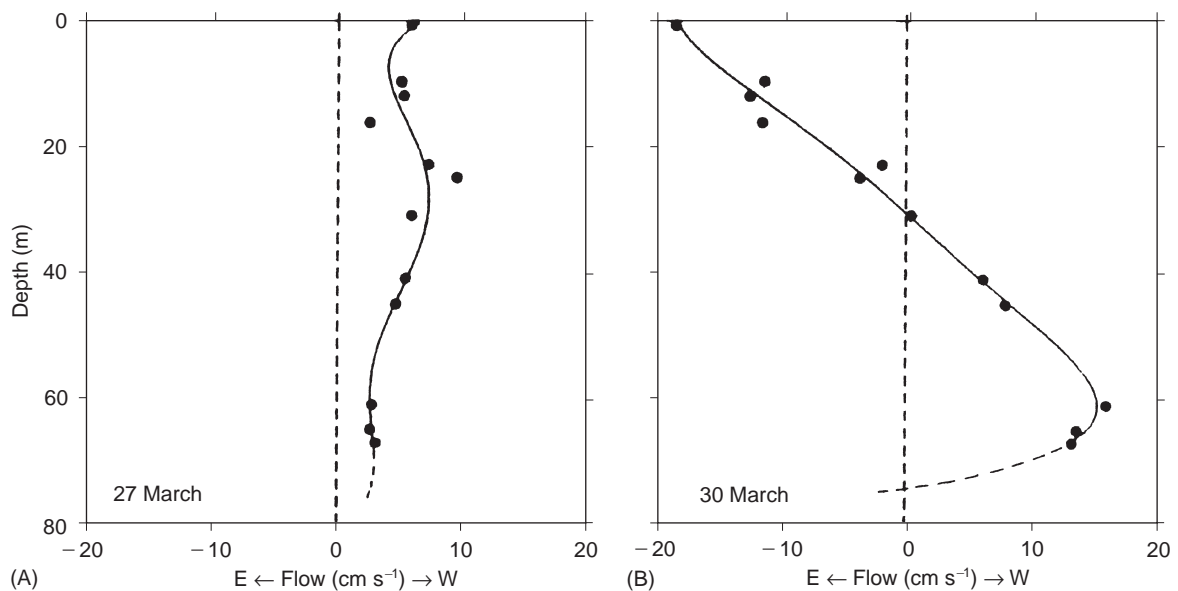
Figure 6 Profiles of cross-shelf flow measured by current meters (solid dots) in 76 m of water on the African continental shelf during (A) near-zero winds and (B) upwelling favorable wind.
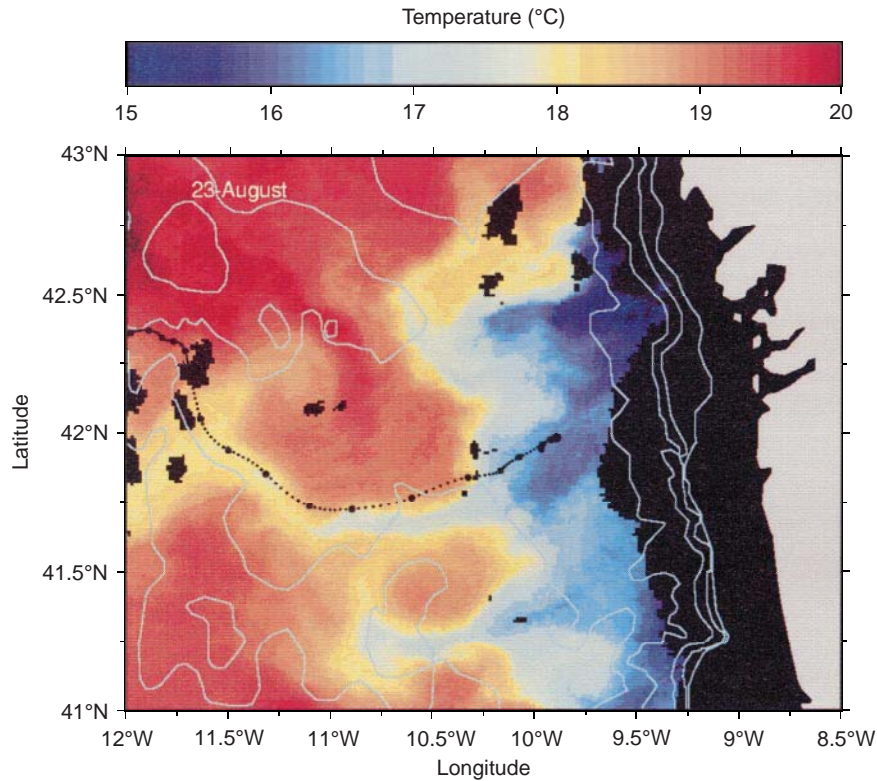
Figure 7 Satellite sea surface temperature image in August showing an upwelling filament extending 200 m offshore. Clouds obscure the image near to shore. A surface layer drift buoy traces the current along the filament. The dots mark daily positions starting on 14 August near shore. White curves mark the 50, 100, 200, 500, and 1000 m isobaths.

Despite many direct and indirect observations of the flow, there are remarkably few systematic observations. The structure of the undercurrent is shown by measurements made close to 20°N (**Figure 8**). Its maximum speed is close to $0.1 \, \text{m s}^{-1}$ at about 150 m below the surface. The core extends about 300–400 m vertically and apparently less than 50 km horizontally (although its offshore limit was not directly observed). Above the undercurrent, shallow equatorward flow predominates, while in layers deeper than 500 m, Antarctic Intermediate Water is carried northward at depths around 900 m. Note also the weak undercurrent in **Figure 5**.

Along most of the eastern subtropical gyre the poleward flow is restricted to the subsurface layers, though it may surface when the Trade Winds weaken or turn northward. Off Iberia and south of 20°N it appears to extend to the sea surface for more of the annual cycle. In the latter area it forms the inshore loop of the cyclonic recirculation. Where it meets the Canary Current separating from the coast, some of the poleward flow continues northward as the undercurrent, carrying with it the typically warmer, fresher, and higher nutrient content South Atlantic Central Water of this region. The anomalous water can be traced as far as the Canary

Islands (28°N) before mixing with the surrounding cooler and saltier North Atlantic Central Water dilutes it beyond recognition. The seasonal analysis showed that during autumn the poleward flow may occur at the sea surface, again reaching the Canary Islands, and the few available direct observations appear to corroborate this.

Off Iberia, most of the water column flows poleward, although the surface layer is flowing equatorward above 200 m depth in the long-term mean. During winter, all of the water column moves northward over the continental slope, but in summer, when the equatorward Trade Winds are present, the currents in the upper few hundred meters are driven equatorward. The undercurrent is known to extend deeply off Iberia, where it carries Mediterranean Intermediate Water at levels between 600 and 1500 m depth. This is water that has escaped through the Strait of Gibraltar and is constrained by the Earth's rotation to flow northward, hugging the continental slope. As it travels northward it tends to separate intermittently from the coast in various locations to form subsurface eddies known as Meddies. Three preferred paths are reported to carry the Mediterranean Water away from the Iberian continental slope: northward where the undercurrent
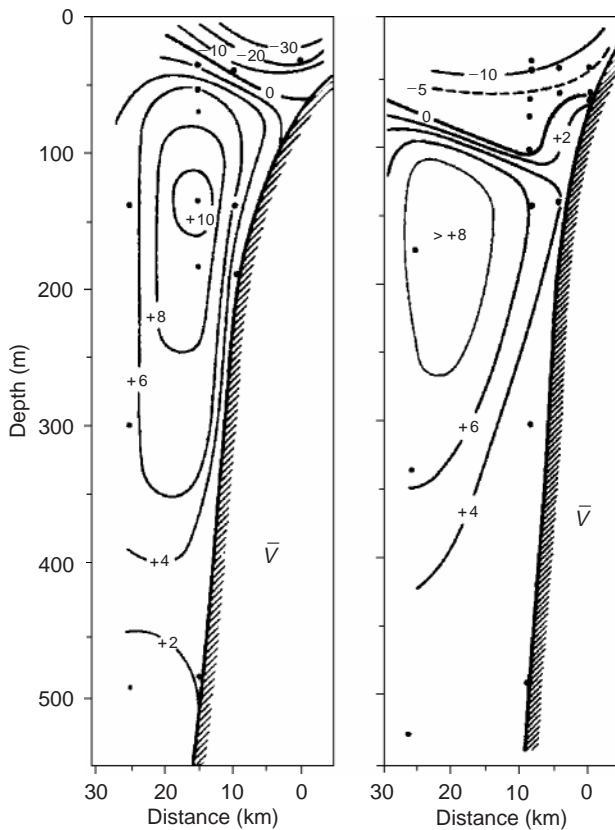
Figure 8 Two sections of alongshore flow measured by current meters (solid dots) near 20°N off north-west Africa, showing structure of the poleward undercurrent. Speeds are given in $cm\,s^{-1}$, northward positive.

extends beyond Cape Finisterre, north-westward west of the Galicia Bank, and south-westward off the Gorringe Bank. In each case the topographic feature seems to trigger the formation of the Meddies, which then migrate away from the boundary and can maintain their identity for up to 4 years.

One unresolved question is whether the poleward flow off NW Africa is in any sense continuous with that off Iberia. There are few observations of the undercurrent off northern Morocco and none that might indicate how the flow interacts with the deepening Mediterranean Intermediate Water. The latter is dense and sinks from shallow levels on leaving the Strait of Gibraltar to its equilibrium level around 1200 m. It therefore must pass through any undercurrent continuing north from Morocco to the Iberian slope in the Gulf of Cadiz.

Spatial Variability

Textbook pictures like **Figure 1** tend to show broad currents of weak unidirectional flows. However, measurements almost always indicate currents

highly variable in both strength and direction. **Figure 9** shows a near-synoptic view of the currents, derived from the combined TOPEX and ERS-1 altimetry on 14 August 1993. The small sea surface height slope anomalies measured by satellites have been added to the mean summer surface elevations calculated with respect to a 400 m reference level from hydrography to compensate in part for the lack of the mean signal in the altimetry. The Azores Current meanders along latitude 32°N, gradually turning southward into the Canary Current. Little flow seems to come from the weak Portugal Current southwards. Near the African coast from 30°N the flow is southward as far as 20°N, where it turns abruptly offshore on meeting poleward flow from farther south. A large number of eddies are seen throughout the region, especially associated with the Azores Current and farther south. The resolution of the altimetry is limited by the ground track separation (~ 50 km or more) and the repeat interval (> 15 days).

A survey of currents just south of the Canary Islands made near the same time (10–18 August 1993) shows patterns of flow on shorter scales as complex as in the satellite view (**Figure 10**). One might ask where the Canary Current is in this complexity. It lies, of course, in the average flow over the area of the survey, about $0.05\,m\,s^{-1}$ toward the south west as expected. However, the instantaneous current in any location can have almost any direction and speed. The flow field is composed of narrow, strong jets of current, which may meander through the area changing their position with time, and eddy circulations that drift with the background flow. Here the alongshore, equatorward flow appears diverted around a 100 km diameter cyclonic eddy generated in the trough of bottom topography between Gran Canaria, Fuerteventura, and Africa. This eddy was only just resolved in the satellite analysis. This level of detail of field observation has only become available in the last two decades with the introduction of acoustic Doppler methods of determining upper-level currents from a moving research vessel. In this way rapid surveys can be made to reveal the intricate patterns of ocean currents, though still in an area limited in size by ship speed.

Numerical Models

Numerical modeling techniques for ocean circulation are improving rapidly as computer power allows more detailed calculations on finer grids. Recent results for the Canary Current region, representing the near-surface flow in early September, are shown in **Figure 11**. The model realistically
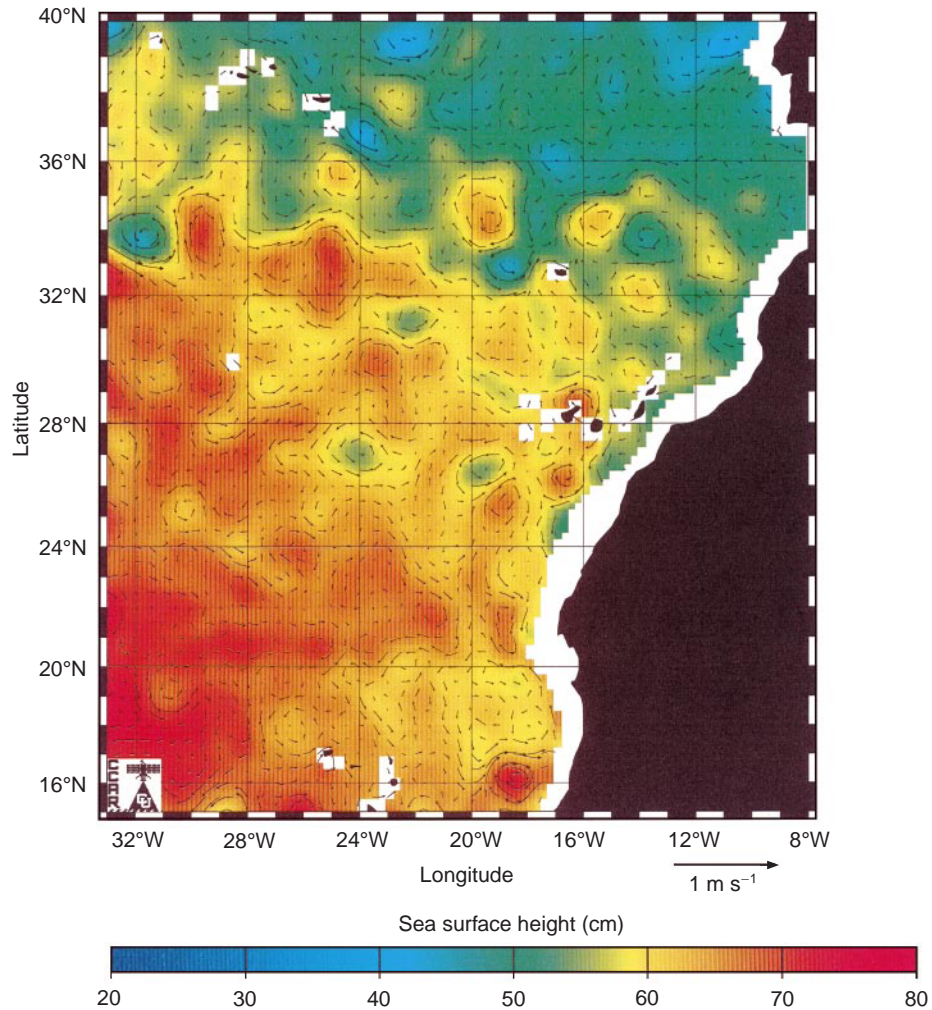
Figure 9   Surface geostrophic currents superimposed on sea surface height fields from TOPEX/ERS-1 altimeter (14 August 1993). The August mean sea surface height calculated from density fields has been added to compensate for lack of altimetric mean.
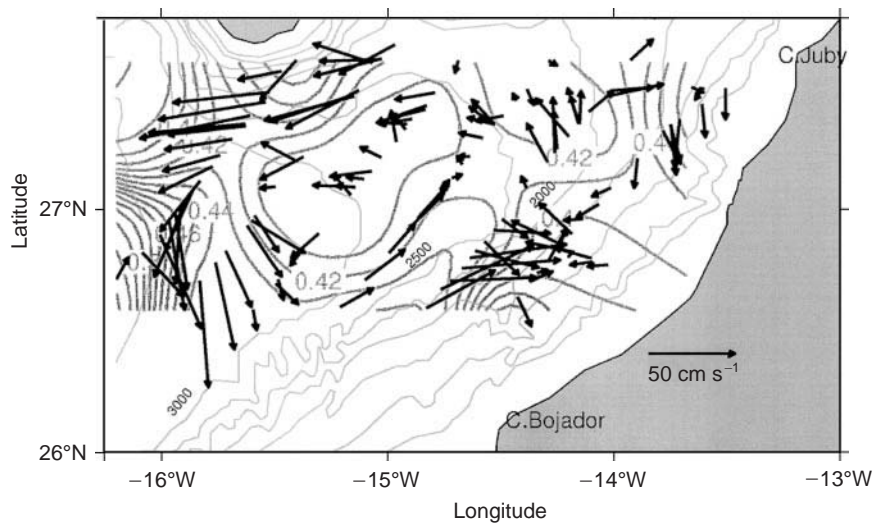
Figure 10   Field of current observed by acoustic Doppler current profiler near the time of **Figure 9**. Sea surface height contours are shown. Note the southward shelf flow turning offshore to describe a cyclonic eddy ∼ 100 km diameter.
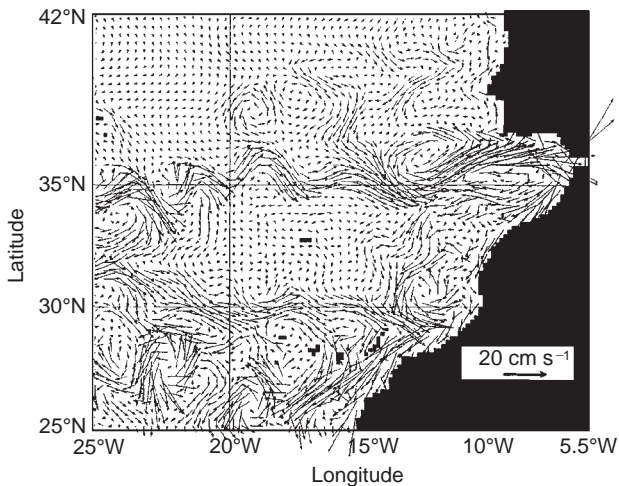
Figure 11 Numerical model results of calculated surface currents for September. (Johnson J and Stevens I 2000 *Deep Sea Research I*, 47(5): 875–900.)

depicts a meandering Azores Current at 35°N, which separates into branches entering the Gulf of Cadiz and flowing south-east into the Canary Current. Note the southward flow near-shore off NW Africa, typical of late summer upwelling conditions, and the prevalence of meanders and eddies throughout the field. Also noteworthy is the near-shore poleward current off Iberia, similar to conditions observed there in September with the cessation of upwelling and onset of the winter season.

This 'state of the art' numerical model is run using climatic winds, i.e., monthly averaged winds that vary smoothly through the year, and has a limited number of layers in the vertical. Nevertheless, the fine horizontal resolution allows the realistic reproduction of oceanic features often only partially sampled because of ship time and equipment constraints. Even this model is on a coarse scale compared to the size of many important features like islands or coastal capes. Entire islands are represented by one or two model grid points so the level of detail does not yet reproduce features on the scales seen in **Figure 10**. In the not too distant future, models driven by actual or forecast winds and incorporating ocean observations from monitoring networks will provide ocean forecasts that will rival in accuracy present-day meteorological models.

Conclusions

The overall features of the Canary and Portugal currents, such as the mean pattern and seasonal variation, are well established despite relatively few systematic observations. The Canary Current is fed from the Azores Current to a lesser extent from the weak Portugal Current. To north and south of the Canary Current proper, regions of predominantly northward flow persist through most of the year. These are apparently connected by a narrow undercurrent trapped to the continental slope near 300 m depth. Variability of the system is dominated by the Trade Wind, which varies on timescales of weeks, seasons, decades, and longer. The Trades directly force coastal upwelling and continental shelf currents throughout the region. Unresolved questions include the reality of the intense equatorward flow alongshore between 30° and 20°N suggested by the seasonal analyses, and the continuity of the undercurrent along the continental margin.

See also

Benguela Current. Canary and Portugal Currents. California and Alaska Currents. Ekman Transport and Pumping. Fisheries and Climate. Mesoscale Eddies. Meddies and Sub-surface Eddies. Regional and Shelf Sea Models. Satellite Altimetry. Satellite Remote Sensing of Sea Surface Temperatures. Upwelling Ecosystems. Water Types and Water Masses. Wind Driven Circulation.

Further Reading

Barton ED (1989) The poleward undercurrent on the eastern boundary of the Subtropical North Atlantic. In: Neshyba S, Smith RL and Mooers CNK (eds) *Poleward Flows Along Eastern Ocean Boundaries*, pp. 82–95. (Springer Lecture Note Series). Berlin: Springer-Verlag.

Barton ED (1998) Eastern boundary of the North Atlantic: Northwest Africa and Iberia. In: Brink KH and Robinson AR (eds) *The Sea*, vol. 11: *The Global Coastal Ocean: Regional Studies and Syntheses*, ch. 22. New York: Wiley.

Brink KH (1997) Wind driven currents over the continental shelf. In: Brink KH and Robinson AR (eds) *The Sea*, vol. 10: *The Global Coastal Ocean: Processes and Methods*, ch. 1. New York: Wiley.

Johnson J and Stevens I (2000) A fine resolution model of the eastern North Atlantic between the Azores, the Canary Islands and the Gibraltar Strait. *Deep-Sea Research* I 47(5): 875–900.

Krauss W (ed) (1996) *The Warmwatersphere of the North Atlantic Ocean*, chs 10–12. Berlin: Borntraeger.

Mann KH and Lazier JRN (1991) *Dynamics of Marine Ecosystems*. Boston: Blackwell.

Mittelstaedt E (1983) The upwelling area off Northwest Africa – a description of phenomena related to coastal upwelling. *Progress in Oceanography* 12: 307–331.

Stramma L and Siedler G (1988) Seasonal changes in the North Atlantic Subtropical Gyre. *Journal of Geophysical Research* 93(C7): 8111–8118.

Tomczak M and Godfrey JS (1994) *Regional Oceanography: An Introduction*. Oxford: Elsevier.